AIP | Journal of Applied Physics

Nonresonant third-order nonlinear properties of NaPO3–WO3–Bi2O3 glasses in the near infrared

F. E. P. dos Santos, C. B. de Araújo, A. S. L. Gomes, K. Fedus, G. Boudebs et al.

Citation: J. Appl. Phys. 106, 063507 (2009); doi: 10.1063/1.3212972
View online: http://dx.doi.org/10.1063/1.3212972
View Table of Contents: http://jap.aip.org/resource/1/JAPIAU/v106/i6
Published by the AIP Publishing LLC.

Nonresonant third-order nonlinear properties of $NaPO_3-WO_3-Bi_2O_3$ glasses in the near infrared

F. E. P. dos Santos,[1] C. B. de Araújo,[1,a)] A. S. L. Gomes,[1] K. Fedus,[2] G. Boudebs,[2] D. Manzani,[3] and Y. Messaddeq[3]
[1]*Departamento de Física, Universidade Federal de Pernambuco, 50670-901 Recife, Pernambuco, Brazil*
[2]*Laboratoire des Proprietés Optique des Materiaux et Applications, Université d'Angers, 49045 Angers Cedex 01, France*
[3]*Instituto de Química, Universidade do Estado de São Paulo (UNESP), 14801-970 Araraquara, São Paulo, Brazil*

(Received 4 July 2009; accepted 30 July 2009; published online 18 September 2009)

The nonlinear (NL) refractive index, n_2, of $NaPO_3-WO_3-Bi_2O_3$ glass with different relative amounts of the constituents was measured at 1064 and 800 nm using the *Z*-scan and the thermally managed eclipse *Z*-scan techniques, respectively. The values of $n_2 \geq 10^{-15}$ cm^2/W and negligible NL absorption coefficient were determined. The large values of the NL refractive index and the very small NL absorption indicate that these materials have large potential for all-optical switching applications. © *2009 American Institute of Physics*. [doi:10.1063/1.3212972]

I. INTRODUCTION

The large interest in photonic devices is motivating the search of new nonlinear (NL) optical materials appropriate for all-optical switching, optical limiting, and frequency generation. For such applications, glassy materials are interesting because their NL optical properties can be tailored by selecting compositions with constituents of large hyperpolarizability.[1–9] Besides the selection of the constituents, the exploitation of composites containing dielectric nanocrystals or metallic nanoparticles is a possible alternative.[10–12] Candidate materials should present also large transmittance for the wavelengths of interest, high mechanical resistance, thermal stability, large linear refractive index, and simple fabrication requirements.

Among the materials already recognized with large potential for photonics, chalcogenide[3,4] and antimony based glasses[7–9] are examples that present appropriate characteristics for devices operating in particular ranges of light wavelength and temporal regimes. On the other hand, tungstate oxide (WO_3) based glasses are emerging as strong candidates for photonic applications. Indeed, photoluminescence studies including frequency upconversion and energy transfer processes involving rare-earth doped tungsten glasses were reported.[13–20] Tungstate-fluorophosphate glasses ($NaPO_3-BaF_2-WO_3$) were investigated because of the large potential of fluorophosphate glasses as laser materials and as optical amplifier media. Besides the demonstration of efficient luminescence behavior of $NaPO_3-BaF_2-WO_3$ doped with rare-earth ions[17] experiments at 660 nm with pulsed lasers[18] showed that they may be used for optical limiting due to their large NL absorption cross section. Third-order NL properties of $NaPO_3-BaF_2-WO_3$ glasses were studied at 532, 800, and 1064 nm with picosecond and femtosecond lasers.[19] For the green wavelength, the NL refractive index, n_2, was $\sim 10^{-15}$ cm^2/W and the NL absorption coefficient, α_2, varied from 0.3 to 0.5 cm/GW for WO_3 concentrations varying from 20% to 50%. The experiments in the infrared did not show relevant NL behavior for WO_3 concentrations smaller than 50%.

In this paper, we report on the third-order nonlinearity of $NaPO_3-WO_3-Bi_2O_3$ glasses that present large NL response in the near infrared. The presence of Bi_2O_3 instead of BaF_2 in the glass composition contributes for the increase in the NL response because of the larger Bi_2O_3 polarizability. The samples prepared have good optical quality, they are stable against moisture, and have large optical damage threshold. The experiments performed in the infrared indicate large values of n_2 for the different compositions investigated. Two variations in the *Z*-scan technique at 1064 and 800 nm, with picosecond and femtosecond laser pulses, respectively, were applied for characterization of the samples. From the experiments, we determine $n_2 \approx 10^{-15}$ cm^2/W, one order of magnitude larger than silica, and negligible NL absorption coefficient. Figures of merit for all-optical switching were determined using the NL parameters measured and the results indicate large potential of $NaPO_3-WO_3-Bi_2O_3$ glasses for photonic devices in the near infrared.

II. EXPERIMENTAL

A. Samples preparation

The glass samples were synthesized by a conventional method. The starting powdered materials were tungsten oxide (WO_3) (99.8% pure), sodium polyphosphate ($NaPO_3$) (99.8% pure), and bismuth oxide (Bi_2O_3) (99.8% pure). In the first step, the powders were mixed and heated at 500 °C for 1 h to remove water and adsorbed gases. Then, the batch was melted at a temperature ranging from 1000 to 1050 °C, depending on the Bi_2O_3 content. The obtained liquid was kept at this temperature for 40 min to ensure homogenization and fining. The influence of the melting time on the physical properties has been reported in Ref. 20. Finally, the melt was

a)Author to whom correspondence should be addressed. Electronic mail: cid@df.ufpe.br.

TABLE I. Compositions and characteristic temperatures of the samples. T_g is the glass transition temperature and T_x refers to the onset of crystallization. The estimated error in the temperature measurements is ±1 °C.

	Glass composition (mol %)			Characteristic temperatures (°C)	
Samples	$NaPO_3$	WO_3	Bi_2O_3	T_g	T_x
FW40B10	50	40	10	471	530
FW30B20	50	30	20	431	513
FW30B15	55	30	15	439	529
FW30B10	60	30	10	433	552
FW30B5	65	30	5	414	571
FW20B15	65	20	15	434	483
FW20B10	70	20	10	398	494
FW20B5	75	20	5	379	506

cooled in a metal mold preheated at 20 °C below the glass transition temperature. Annealing was implemented at this temperature for 2 h in order to minimize mechanical stress resulting from thermal gradients upon cooling. The bulk samples were cut and polished before performing the optical measurements. The actual composition of the samples and their characteristic temperatures are given in Table I.

B. The *Z*-scan setup

The picosecond third-order nonlinearity was investigated using the *Z*-scan technique[21,22] and Fig. 1 shows the setup used. The excitation is provided by a linearly polarized mode-locked neodymium-doped yttrium aluminum garnet (Nd:YAG) laser (1064 nm, pulse duration of 17 ps, and repetition rate of 10 Hz). The laser beam is focused by a lens L_1 with focal distance $f_1=20$ cm and the beam waist radius at the focal plane is $w_0=30$ μm corresponding to a Rayleigh length of ≈3 mm. The measurements were performed using a $4f$ system with incident intensities on the samples varying from 3 to 35 GW/cm^2 [the calibration process was performed using CS_2 as a reference sample assuming $n_2=3.0\times10^{-18}$ m^2/W (Ref. 21)]. The image receiver is a 1000 ×1800 pixel charge coupled device (CCD) cooled camera operating at −30 °C with a fixed gain. The camera is placed at a distance equal to f_2 (20 cm), the focal length of lens L_2. A reference beam incident on a small area of the camera allows to monitor the energy fluctuation of the laser pulses to

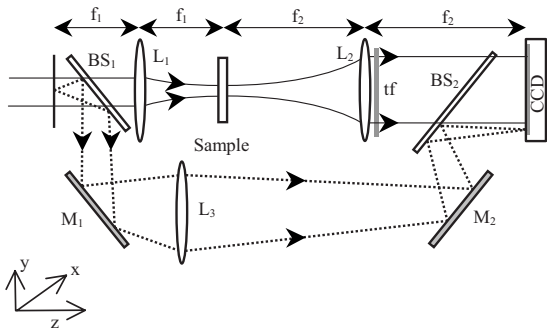

FIG. 1. Experimental *Z*-scan setup. The labels refer to lenses (L_1–L_3), mirrors (M_1,M_2), beam splitters (BS_1,BS_2), and neutral filters (tf). The sample is moved in the focal region between L_1 and L_2.

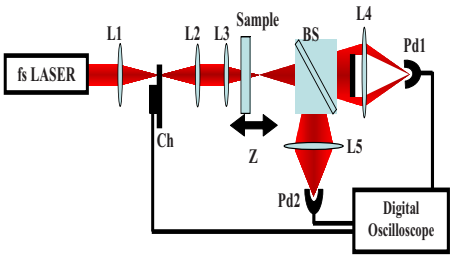

FIG. 2. (Color online) Experimental TM-EZ scan setup. The labels refer to lenses (L_1–L_5), beam splitter (BS), photodiodes (Pd1, Pd2), and chopper (Ch).

take into account the intensity changes in the calculation of the NL parameters. The sample is scanned in the focus region along the beam propagation direction (z axis) as in the original *Z*-scan experiment.[21] *Open aperture* and *closed aperture* normalized transmittance were numerically processed from the acquired CCD images by integrating over all camera pixels in the first case and over a circular numerical filter in the second case (corresponding to a linear aperture transmittance $S=0.4$). Lens L_2 contributes to produce the Fourier transform of the field at the exit surface of the sample, which is physically similar to the far-field diffraction obtained with the original *Z*-scan method. Equation 13 of Ref. 19 relating the NL parameters to ΔT_{PV}, the difference between the normalized peak and valley transmittances, remains valid for the $4f$ system used here.

C. Thermally managed eclipse *Z*-scan technique

The thermally managed eclipse *Z*-scan (TM-EZ scan) technique was recently introduced for measurements of the electronic nonlinearity of materials using high repetition pulsed lasers.[23] It is a variation of the technique introduced in Ref. 24 to differentiate between thermal and nonthermal nonlinearities. The eclipse *Z*-scan scheme makes the setup more sensitive to small NL signals and therefore smaller laser intensities can be used. The setup used in this work is illustrated in Fig. 2. A mode-locked Ti-sapphire laser (800 nm, pulse duration of 150 fs, and repetition rate of 76 MHz) was employed in the experiments. A disk with diameter of 1.7 cm was placed in front of a 10 cm focal distance lens (L_4) to direct the eclipsed beam to the detector. About 1% of the transmitted beam through the sample reaches the Pd1 detector. The NL measurements are made by acquiring the time evolution of the *Z*-scan signal for the sample placed in the prefocal and postfocal positions with respect to lens L_3. The time resolution (18 μs), determined by the chopper opening time ($t=0$) depends on the finite size of the beam waist on the chopper wheel. The time evolution of the *Z*-scan signal is obtained by delaying the photodetector signal acquisition time with respect to $t=0$. From these measurements, using the theoretical procedure of Ref. 21, the *Z*-scan curves can be constructed and the contribution of thermal (slow) and nonthermal (fast) nonlinearities can be inferred.[23,24] Curves representing the transmittance as a function of time (when the sample is in the peak and in the valley positions) are constructed. A rise or decay time and crossing of the two curves (corresponding to the pre- and postfocal signals) in-

TABLE II. Linear refractive indices of the samples.

	Wavelength (nm)		
Sample	532	633	1538
FW40B10	1.8570	1.8381	1.7979
FW30B20	1.8950	1.8748	1.8323
FW30B15	1.7924	1.7770	1.7434
FW30B10	1.7815	1.7660	1.7330
FW30B5	1.7006	1.6891	1.6622
FW20B15	1.7305	1.7151	1.6987
FW20B10	1.7171	1.7050	1.6765
FW20B5	1.7144	1.7022	1.6745

dicate the presence of thermal and nonthermal (electronic) nonlinearity with contributions of opposite signs.[23,24] When the signs of both nonlinearities are the same, the transmittance curves do not cross but they grow with time. Flat temporal evolution curves indicate the absence of thermal contribution.

III. RESULTS AND DISCUSSIONS

The samples present large transmittance window from ≈400 to ≈2000 nm having a linear absorption coefficient smaller than 2.5 cm^{-1}. Table II shows the values for the linear refractive index, n_0, measured at 532, 632.8, and 1538 nm using the *M*-line technique. This technique provides measurements of n_0 with five digits that represent a larger accuracy than it is required for the interpretation of the NL experiments. The values in Table II indicate that n_0 increases with the concentrations of WO_3 and Bi_2O_3.

Figures 3(a) and 3(b) show the *Z*-scan profiles obtained using the Nd: YAG laser at 1064 nm (pulses of 17 ps) for three representative samples. The experiments with the other samples show analogous behavior and similar signal-to-noise ratios. The closed aperture *Z*-scan profiles indicate positive values of n_2 for all samples. In all cases, the NL absorption coefficient, α_2, is very small and remains under the detection limit of the measurement system for the majority of the samples.

Figures 4(a)–4(d) show the closed aperture TM-EZ scan results (profile and the time evolution) corresponding to samples FW30B15 and FW20B10. The EZ scan profiles with prefocal peak and postfocal valley indicate self-focusing nonlinearity for all samples. The temporal behavior of the signals, without crossing of the lines corresponding to prefocal and postfocal transmission signals in Figs. 4(b) and 4(d), shows that slow contributions are negligible in the present experimental conditions. This is an indication that thermal effects and contributions due to long lifetime states are negligible. The positive values of n_2 corroborate that the NL response is dominated by the electronic contribution. The NL absorption coefficients of the samples were smaller than the minimum value that our setup allows to measure (0.01 cm/GW). Extrapolation of the curves of Figs. 4(b) and 4(d) to $t=0$ allows the determination of n_2 of electronic origin.

Calculations of n_2 and α_2 for all samples were made following the procedure of Ref. 21 and the results are given

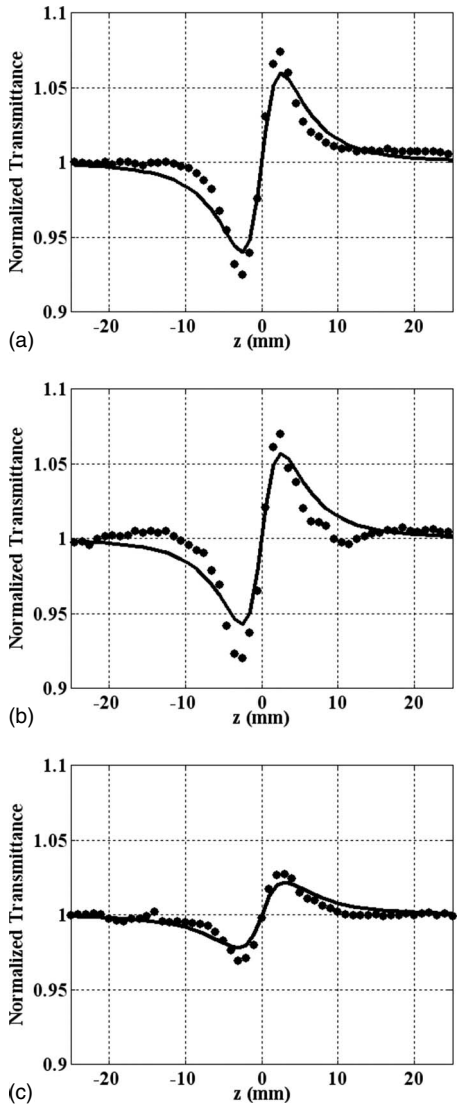

FIG. 3. Closed-aperture *Z*-scan transmittances at 1064 nm. Experimental results (points) and theoretical fits (solid lines) for samples: (a) FW30B5 (thickness of 1.23 mm and $I_0=36$ GW/cm^2); (b) FW30B15 (thickness: 1.72 mm; $I_0=20$ GW/cm^2); (c) FW30B10, (thickness: 3.70 mm; $I_0=4.5$ GW/cm^2). I_0 is the on-axis peak intensity at the focus of lens L_1 of Fig. 1.

in Table III for 1064 and 800 nm. Note that n_2 is positive at both wavelengths for all glass compositions and their values are typically one order of magnitude larger than for silica.[25] As mentioned before, the values of α_2 are negligible for both wavelengths.

Examining Table III, it can be verified that WO_3 and Bi_2O_3 contribute for n_2 because its value increases with the sum of the concentrations of WO_3 and Bi_2O_3. The contribution of WO_3 for the NL response is attributed to the high hyperpolarizability associated with the W–O bonds,[19] while the contribution of Bi_2O_3 is due to the large hyperpolarizability of the Bi–O–Bi bonds.[26,27]

The figure of merit for all-optical switching, $T=2\alpha_2\lambda/n_2$, was calculated and values of T smaller than 0.5 were obtained in the picosecond regime at 1064 nm. In the femtosecond regime at 800 nm, T is smaller than 1.4. The results indicate that $NaPO_3$–WO_3–Bi_2O_3 glasses can be

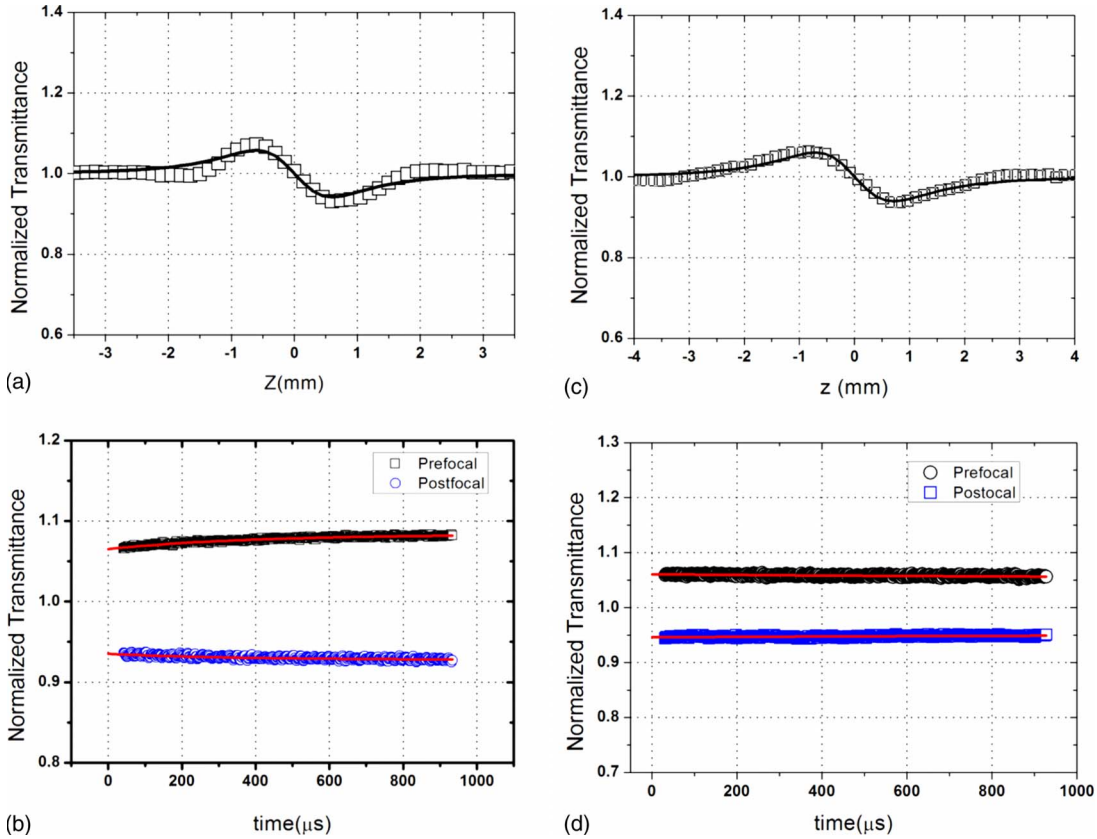

FIG. 4. (Color online) Closed-aperture TM-EZ scan results at 800 nm. [(a) and (c)] Profiles corresponding to samples FW30B15 (thickness of 1.72 mm) and FW20B10 (thickness of 2.18 mm), respectively. [(b) and (d)] temporal behavior of the signals corresponding to prefocal and postfocal signals, respectively. On-axis peak intensity at the focus of lens L_3 of Fig. 2: $I_0=2.63$ GW/cm^2.

used in devices such as directional couplers and NL distributed feedback gratings that require $T<1$ and $T<4$, respectively.[28]

IV. CONCLUSION

The large NL refractive index and low NL absorption coefficient of the glass samples studied demonstrate their large potential for photonic applications. Clearly the results indicate that $NaPO_3-WO_3-Bi_2O_3$ glasses are good candidates for all-optical switching devices operating in the near infrared. The figure of merit, $T=2\alpha_2\lambda/n_2$, for all-optical switching presents the values that satisfy the requirements established in the literature. Moreover, another indication that $NaPO_3-WO_3-Bi_2O_3$ glasses can be useful for photonics is the fact that optical fibers were produced from performs having the compositions reported here.[29] Fibers with good optical quality were obtained and their characterization will be published elsewhere.

TABLE III. NL parameters: n_2 is the NL refractive index and α_2 is the two-photon absorption coefficient.

	Picosecond regime (1064 nm)		Femtosecond regime (800 nm)	
Samples	n_2 (10^{-16} cm^2/W)	α_2 (cm/GW)	n_2 (10^{-16} cm^2/W)	α_2 (cm/GW)
FW40B10	36 ± 6	<0.03	⋯	⋯
FW30B20	30 ± 4	<0.01	11 ± 2	<0.01
FW30B15	22 ± 3	<0.01	8 ± 1	<0.01
FW30B10	17 ± 2	<0.01	⋯	⋯
FW30B5	16 ± 2	<0.01	8 ± 1	<0.01
FW20B15	19 ± 3	0.013 ± 0.007	10 ± 2	<0.01
FW20B10	15 ± 2	0.027 ± 0.007	15 ± 2	<0.01
FW20B5	15 ± 3	<0.01	8 ± 1	<0.01

ACKNOWLEDGMENTS

This work was supported by the National Institute of Photonics (INCT Photonics). We acknowledge the financial support of the Brazilian agencies: Conselho Nacional de Desenvolvimento Científico e Tecnológico (CNPq), Fundação de Amparo à Ciência e Tecnologia do Estado de Pernambuco (FACEPE), and the CAPES/COFECUB program of international cooperation.

[1] See, for instance, M. Yamane and Y. Asahara, *Glasses for Photonics* (Cambridge University Press, Cambridge, UK, 2000).
[2] K. Tanaka, J. Mater. Sci.: Mater. Electron. **16**, 633 (2005).
[3] R. A. H. El-Mallawany, *Tellurite Glasses Handbook: Physical Properties and Data* (CRC, Boca Raton, FL, 2002).
[4] A. Zakery and S. R. Elliott, *Optical Nonlinearities in Chalcogenide Glasses and their Applications*, Springer Series in Optical Sciences (Springer, Berlin, 2007).
[5] G. S. Maciel, N. Rakov, C. B. de Araújo, A. A. Lipovskii, and D. K. Tagantsev, Appl. Phys. Lett. **79**, 584 (2001).
[6] D. Munoz-Martin, H. Fernandez, J. M. Fernandez-Navarro, J. Gonzalo, J. Solis, J. L. G. Fierro, C. Domingo, and J. V. Garcia-Ramos, J. Appl. Phys. **104**, 113510 (2008).
[7] E. L. Falcão-Filho, C. B. de Araújo, C. A. C. Bosco, G. S. Maciel, and L. H. Acioli, J. Appl. Phys. **97**, 013505 (2005).

[8]L. A. Gómez, C. B. de Araújo, D. N. Messias, L. Misoguti, S. C. Zílio, M. Nalin, and Y. Messaddeq, J. Appl. Phys. **100**, 116105 (2006).
[9]L. A. Gómez, C. B. de Araújo, R. Putvinskis, Jr., S. H. Messaddeq, Y. Ledemi, and Y. Messaddeq, Appl. Phys. B: Lasers Opt. **94**, 499 (2009).
[10]L. A. Gómez, F. E. P. dos Santos, A. S. L. Gomes, C. B. de Araújo, L. R. P. Kassab, and W. G. Hora, Appl. Phys. Lett. **92**, 141916 (2008).
[11]L. Irimpan, V. P. N. Nampoori, and P. Radhakrishnan, Chem. Phys. Lett. **455**, 265 (2008).
[12]G. Piredda, D. D. Smith, B. Wendling, and R. W. Boyd, J. Opt. Soc. Am. B **25**, 945 (2008).
[13]P. Subbalakshmi and N. Veeraiah, J. Phys. Chem. Solids **64**, 1027 (2003).
[14]P. Subbalakshmi, B. V. Raghavaiah, R. B. Rao, N. Veeraiah, P. Babu, and C. K. Jayasankar, Eur. Phys. J.: Appl. Phys. **26**, 169 (2004).
[15]Y. Luo, J. Zhang, J. Sun, S. Lu, and X. Wang, Opt. Mater. (Amsterdam, Neth.) **28**, 255 (2006).
[16]G. Poirier, M. Nalin, L. Cescato, Y. Messaddeq, and S. J. L. Ribeiro, J. Chem. Phys. **125**, 161101 (2006).
[17]G. Poirier, V. A. Jerez, C. B. de Araújo, Y. Messaddeq, S. J. L. Ribeiro, and M. Poulain, J. Appl. Phys. **93**, 1493 (2003).
[18]G. Poirier, C. B. de Araújo, Y. Messaddeq, S. J. L. Ribeiro, and M. Poulain, J. Appl. Phys. **91**, 10221 (2002).
[19]E. L. Falcão-Filho, C. B. de Araújo, C. A. C. Bosco, L. H. Acioli, G. Poirier, Y. Messaddeq, G. Boudebs, and M. Poulain, J. Appl. Phys. **96**, 2525 (2004).
[20]G. Poirier, M. Poulain, Y. Messaddeq, and S. J. L. Ribeiro, J. Non-Cryst. Solids **351**, 293 (2005).
[21]M. Sheik-Bahae, A. A. Said, T. H. Wei, D. J. Hagan, and E. W. van Stryland, IEEE J. Quantum Electron. **26**, 760 (1990).
[22]K. Fedus, G. Boudebs, C. B. de Araújo, M. Cathelinaud, F. Charpentier, and V. Nazabal, Appl. Phys. Lett. **94**, 061122 (2009).
[23]A. S. L. Gomes, E. L. Falcão-Filho, C. B. de Araújo, D. Rativa, and R. E. de Araujo, Opt. Express **15**, 1712 (2007).
[24]A. Gnoli, L. Razzari, and M. Righini, Opt. Express **13**, 7976 (2005).
[25]D. Milam, Appl. Opt. **37**, 546 (1998).
[26]N. Sugimoto, H. Kanbara, S. Fujivara, K. Tanaka, and K. Hirao, J. Opt. Soc. Am. B **16**, 1904 (1999).
[27]H. Nasu, T. Ito, H. Hase, J. Matsuoka, and K. Kamiya, J. Non-Cryst. Solids **204**, 78 (1996).
[28]G. I. Stegeman, in *Nonlinear Optics of Organic Molecules and Polymers*, edited by H. S. Nalva and S. Miyata (CRC, Boca Raton, FL, 1997), p. 799.
[29]Y. Messaddeq (unpublished).